Supporting Information for:

Electrochemiluminescence detection of reduced and oxidized glutathione

ratio by quantum dot-layered double hydroxide film

Yingchang Yu, Jingjing Shi, Xiaocen Zhao, Zhiqin Yuan,* Chao Lu* and Jun Lu

State Key Laboratory of Chemical Resource Engineering, Beijing University of Chemical Technology, Beijing 100029, China. Fax/Tel: 86 010 64411957

The detail of computation

The density functional theory (DFT) with Becke's three parameter (B3)[1] exchange functional along with the Lee-YangParr (LYP)[2,3] nonlocal correlation functional (B3LYP) and an efficient 6-31G basis sets have been applied in our study. The ground state configuration of cysteine (Cys), glutathione (GSH) and glutathione disulfide (GSSG) have been optimized using the aforementioned theoretical level without any symmetry restriction. The frequency calculation has been employed to verify that computed consequences were rational. All above-mentioned calculations were implemented by the Gaussian 09 software.[4]

Oxygen atoms correspond to the red balls, carbon atoms represent as the gray balls, sulfur atoms stand for the yellow balls, nitrogen atoms describe as the blue balls, hydrogen atoms depict as the white balls, aluminum atoms consider as the pink octahedron and magnesium atoms regard as the green octahedron.

In order to further study the interaction mechanism between ZnAl-LDH nanosheets and organic molecules, molecular simulation were performed using the Universal molecular mechanics force fields through the Forcite module of Accelrys Materials Studio 5.5 software. For geometry optimization, the convergence tolerance is employed using customized quality with energy convergence 1×10^{-3} kcal/mol and displacement 1.5×10^{-2} Å. The non-bond energy of GSH was -552.99 kJ/mol, less than that of GSSG (-589.04 kJ/mol) and Cys (-3639.27 kJ/mol), which was in agreement with experiment results.

References

(1) A. D. Becke, *J. Chem. Phys.* 1993, **98**, 5648-5652.

(2) C. Lee, W. Yang and R. G. Parr, *Phys. Rev. B* 1988, **37**, 785-789.

(3) B. Miehlich, A. Savin, H. Stoll and H. Preuss, *Chem. Phys. Lett.* 1989, **157**, 200-206.

(4) M. J. Frisch, G. W. Trucks, H. B. Schlegel, G. E. Scuseria, M. A. Robb, J. R. Cheeseman, G. Scalmani, V. Barone, B. Mennucci, G. A. Petersson, H. Nakatsuji, M. Caricato, X. Li, H. P. Hratchian, A. F. Izmaylov, J. Bloino, G. Zheng, J. L. Sonnenberg, M. Hada, M. Ehara, K.

Toyota, R. Fukuda, J. Hasegawa, M. Ishida, T. Nakajima, Y. Honda, O. Kitao, H. Nakai, T. Vreven, J. A. Montgomery, P. E. Peralta, F. Ogliaro, M. Bearpark, J. J. Heyd, E. Brothers, K. N. Kudin, V. Nn. Staroverov, R. Kobayashi, J. Normand, K. Raghavachari, A. Rendell, J. C. Burant, S. S. Iyengar, J. Tomasi, M. Cossi, N. Rega, N. J. Millam, M. Klene, J. E. Knox, J. B. Cross, V. Bakken, C. Adamo, J. Jaramillo, R. Gomperts, R. E. Stratmann, O. Yazyev, A. J. Austin, R. Cammi, C. Pomelli, J. W. Ochterski, R. L. Martin, K. Morokuma, V. G. Zakrzewski, G. A. Voth, P. Salvador, J. J. Dannenberg, S. Dapprich, A. D. Daniels, Ö. Farkas, J. V. Ortiz, J. Cioslowski, D. Fox, *J. Gaussian 09, revision C.01; Gaussian Inc.: Wallingford, CT,* 2009.

Table. S1. The zeta potential of QDs mixture and ZnAl-LDH nanosheets.

Samples	zeta potential (mV)
QDs mixture	-34.2
ZnAl-LDH nanosheets	29.5
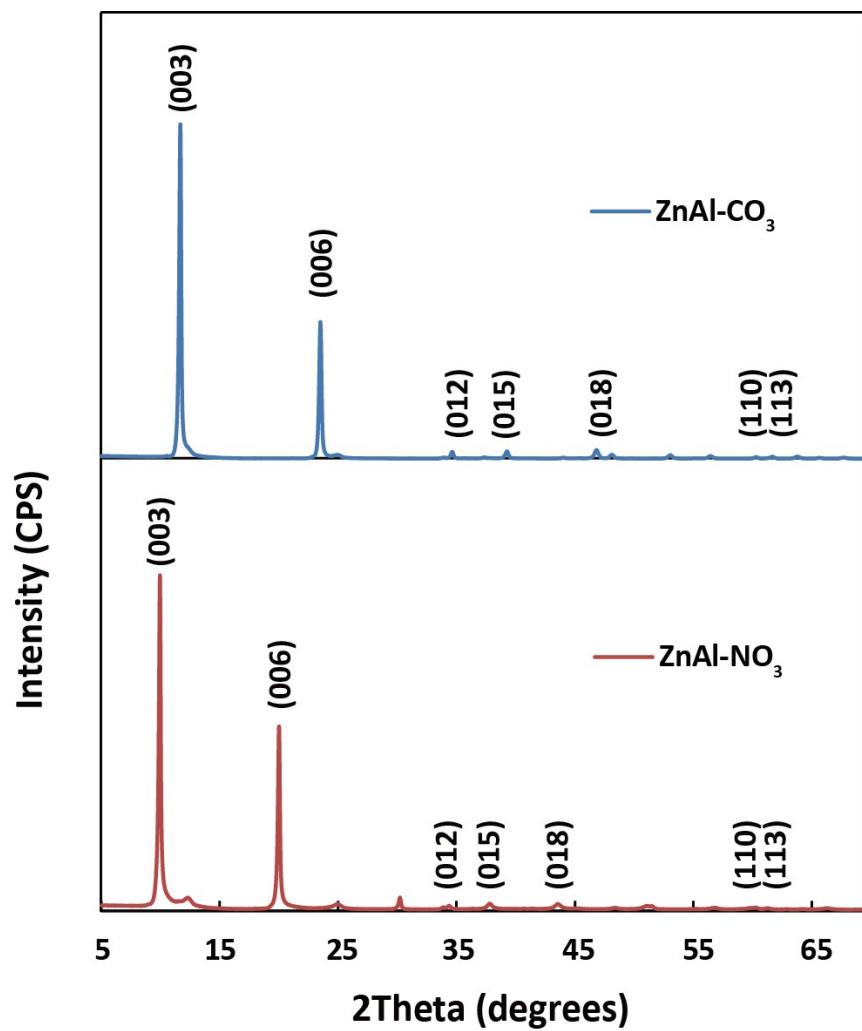
Fig. S1. Power XRD patterns of the (a) ZnAl-CO$_3$ LDHs, (b) ZnAl-NO$_3$ LDHs.
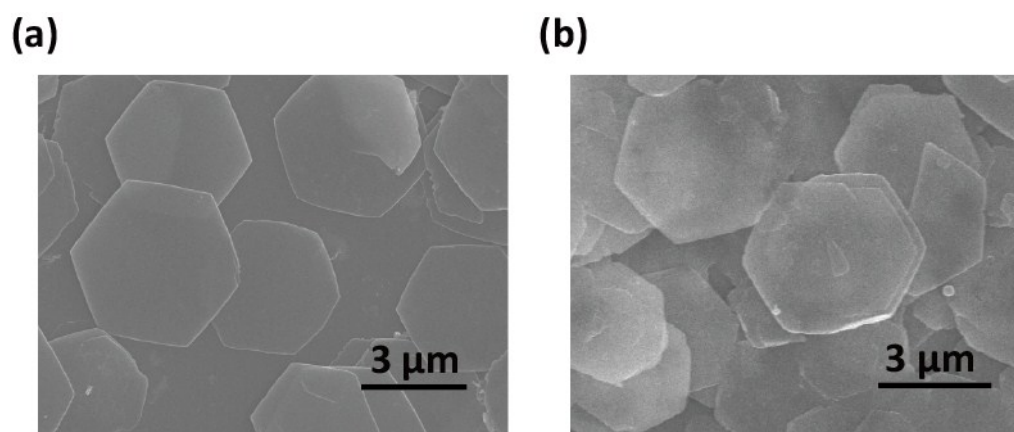
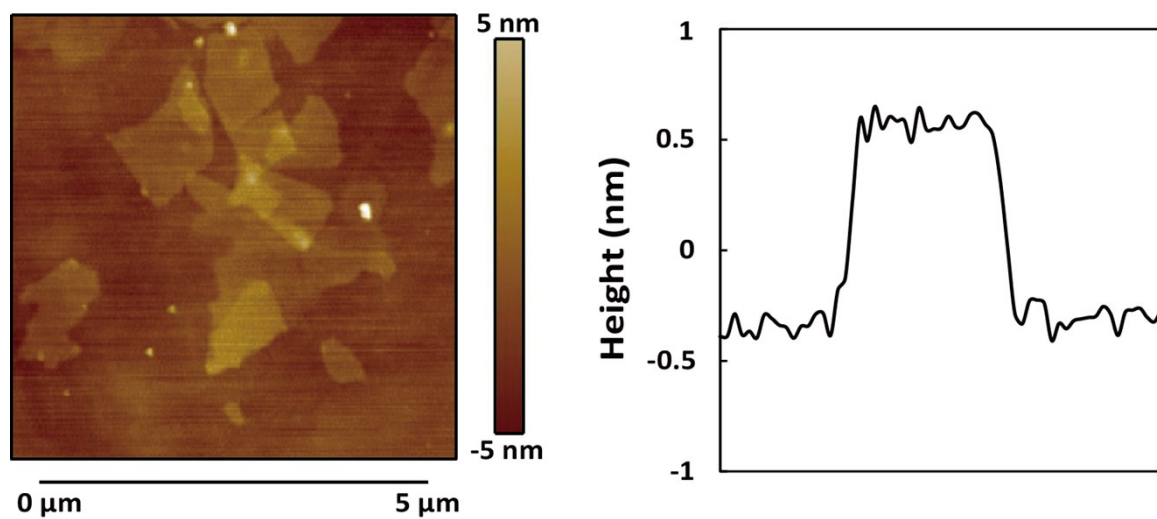**Fig. S2.** SEM images of the (a) ZnAl-CO$_3$ LDHs and (b) ZnAl-NO$_3$ LDHs.

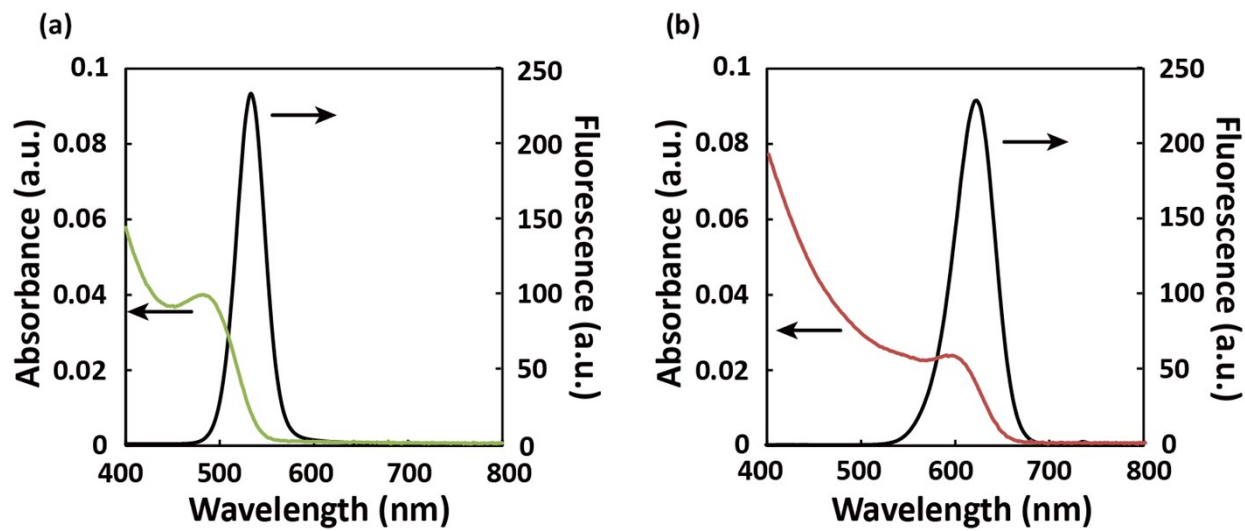**Fig. S3.** AFM image of the exfoliated ZnAl−LDH nanosheets which deposited on a fresh silicon substrate slice.

Fig. S4. The absorption and fluorescence spectra of (a) green QDs and (b) red QDs.
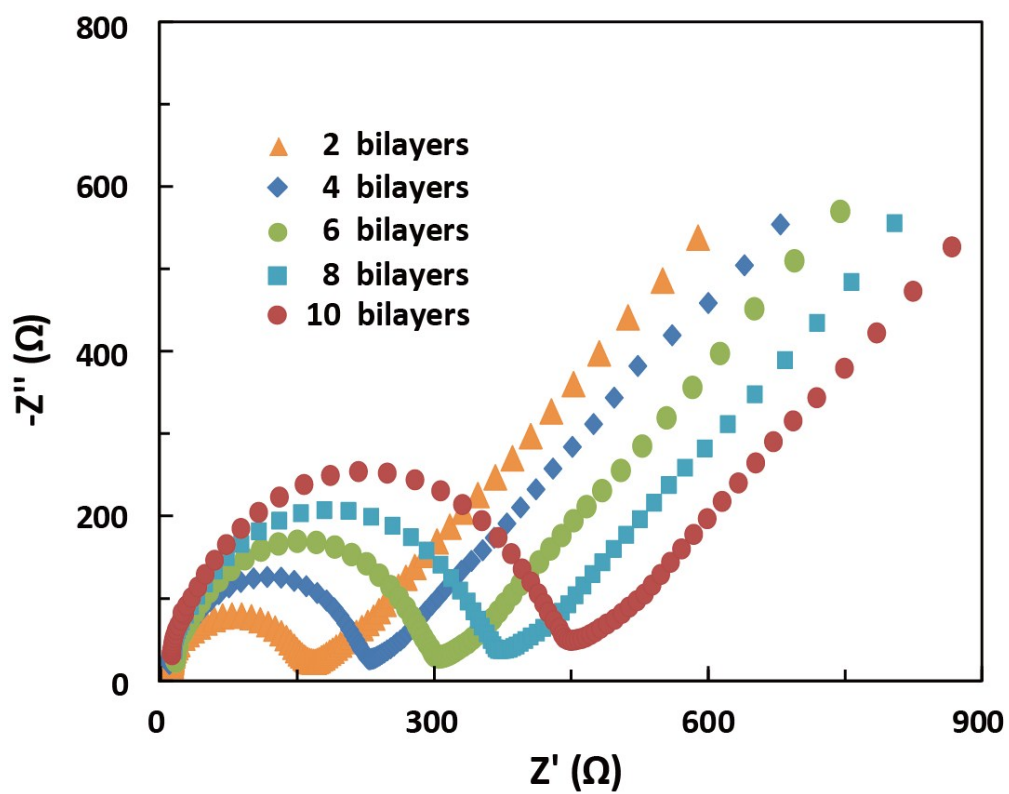
Fig. S5. Nuguist plots of electrochemical impedance spectroscopy for the PDDA/(Mixture/ZnAl-LDH)$_n$ multilayer films modified glassy carbon electrodes with different bilayer number (n) : 2, 4, 6, 8 and 10.
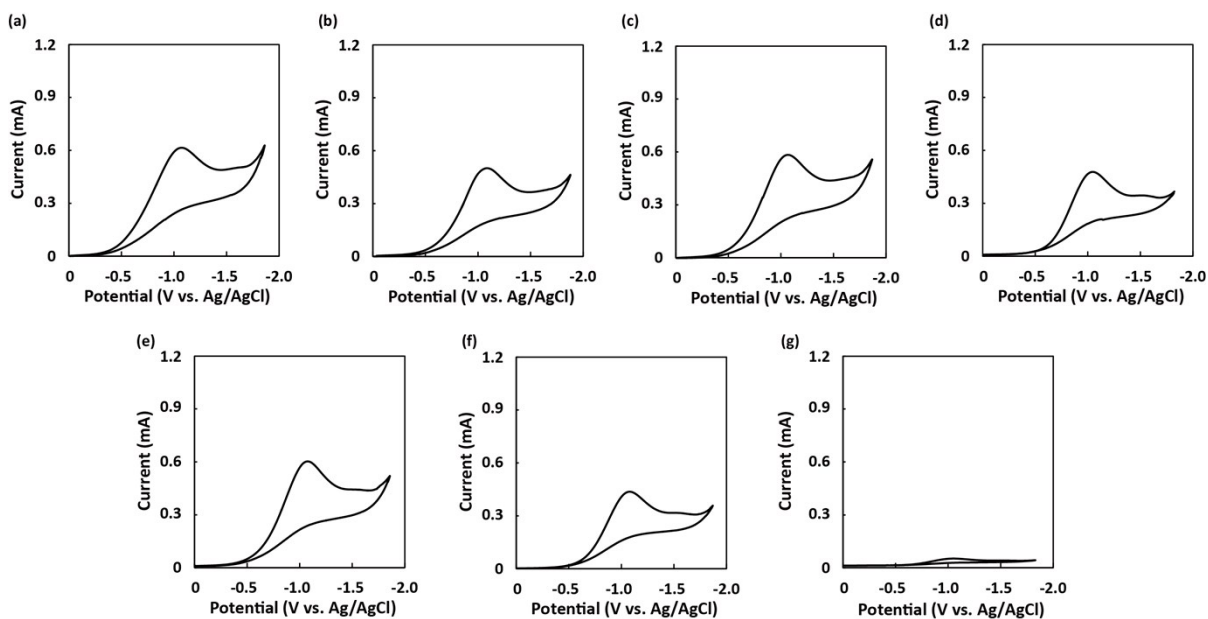
Fig. S6. Cyclic voltammograms of (a) PDDA/(Mixture/ZnAl-LDH)$_6$, (b) Mixture, (c) PDDA/(QDs$_{\lambda em=535}$/ZnAl-LDH)$_6$, (d) QDs$_{\lambda em=535}$ (e) PDDA/(QDs$_{\lambda em=620}$/ZnAl-LDH)$_6$, (f) QDs$_{\lambda em=620}$ modified GC electrodes and (g) bare GC electrode.
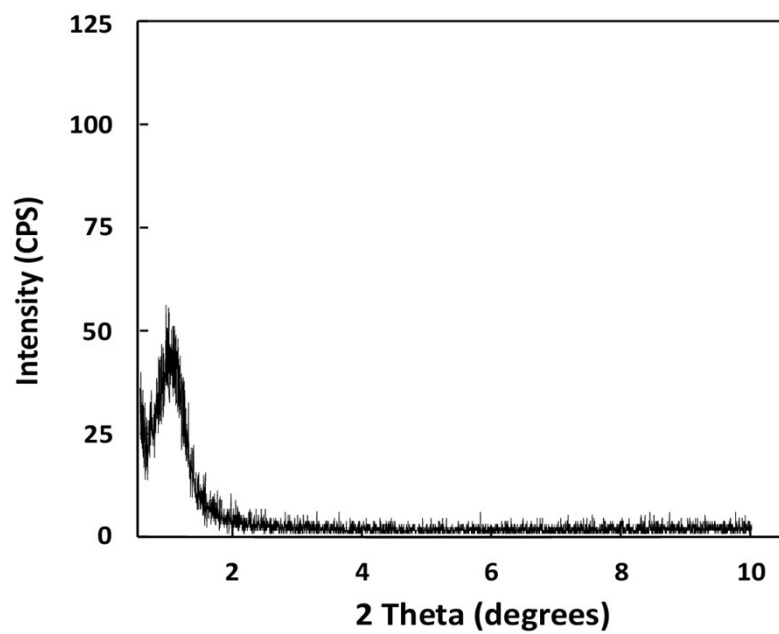
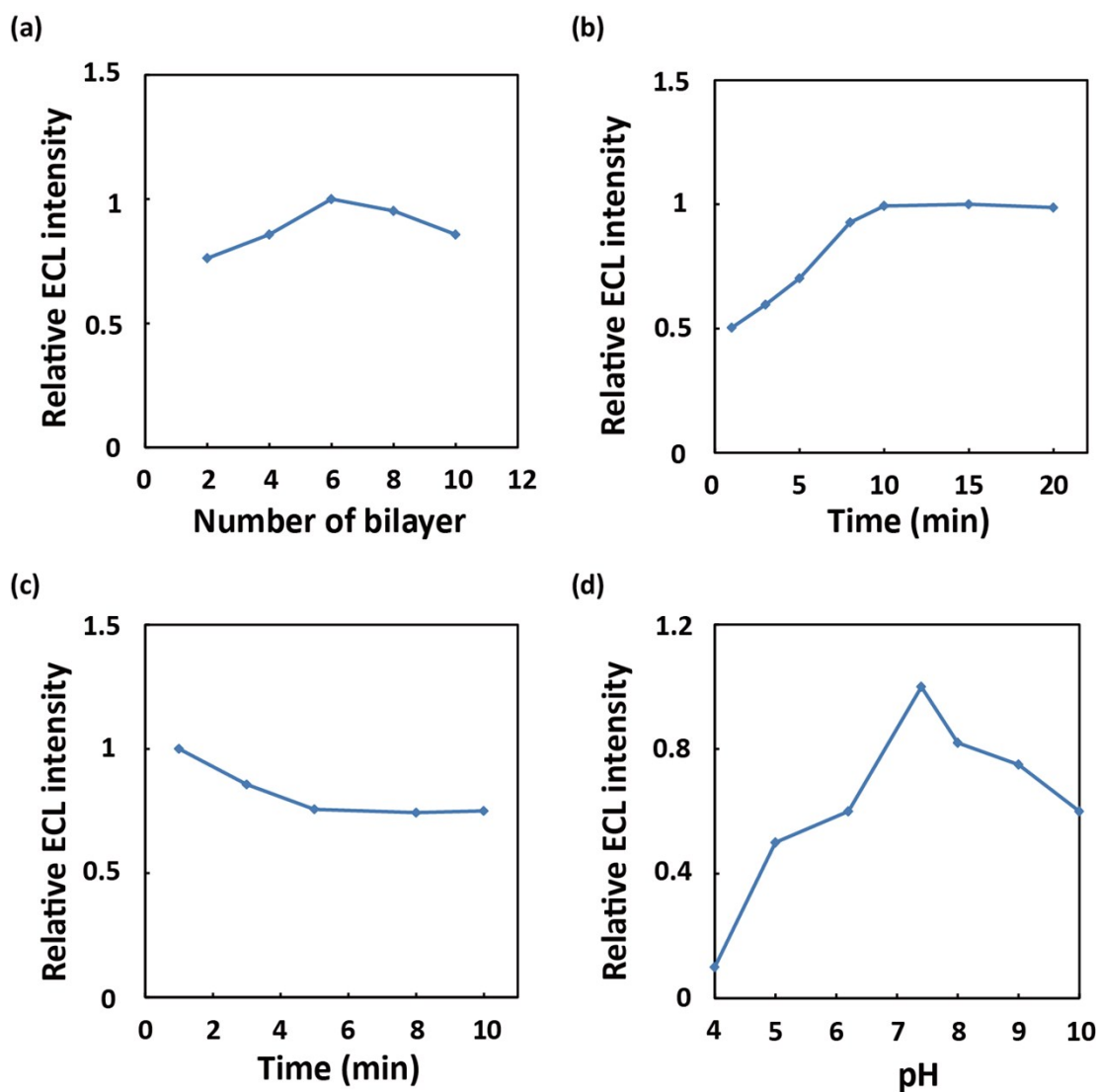**Fig. S7.** The XRD patterns for the PDDA/(Mixture/ZnAl-LDH)$_6$ multilayer films.

Fig. S8. Relative ECL intensity of the PDDA/(Mixture/ZnAl-LDH)$_n$ multilayer films modified glassy carbon electrodes as a function of (a) number of bilayer, (b) QDs adsorption time, (c) LDH nanosheets adsorption time and (d) pH value in 0.1 M PBS (pH=7.4) with 50 mM Na$_2$S$_2$O$_8$. Scanning rate: 100 mV/s.
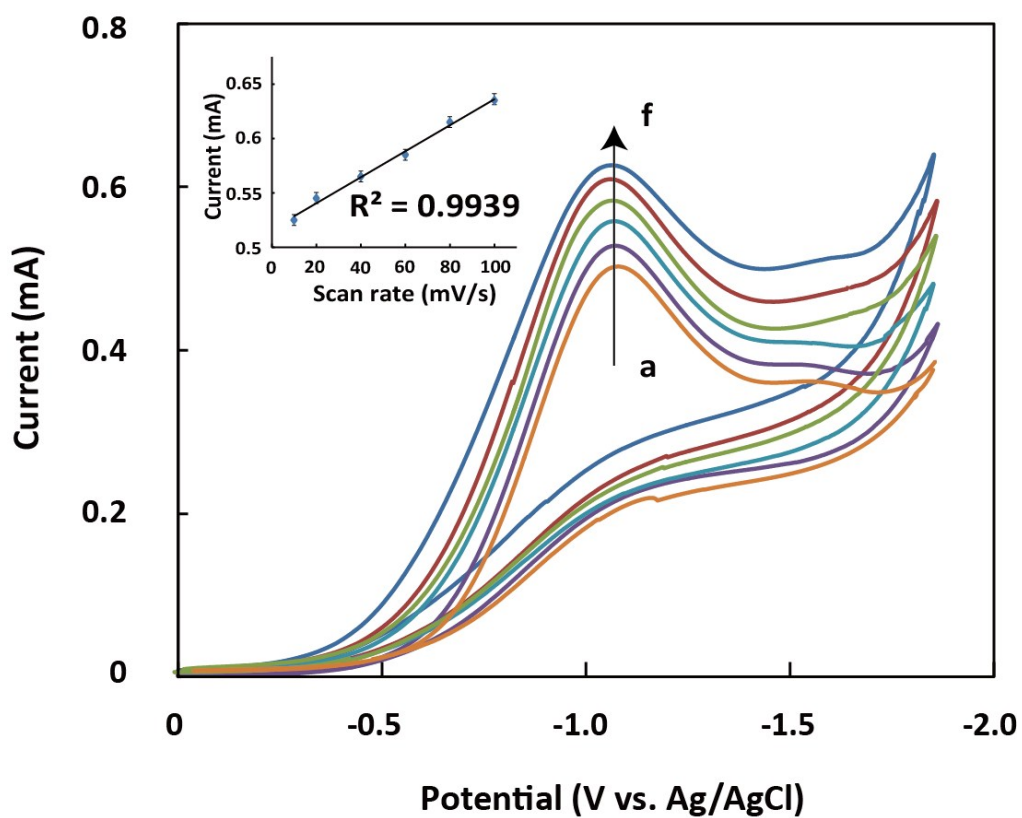
Fig. S9. The cyclic voltammograms (CV) curves of the PDDA/(Mixture/ZnAl-LDH)$_6$ multilayer films modified glassy carbon electrodes in 0.1 M PBS solution (pH=7.4) with 50 mM Na$_2$S$_2$O$_8$ at various scan rates (a) 10, (b) 20, (c) 40, (d) 60, (e) 80 and (f) 100 mV/s. Inset: plots of peak current vs. scan rate.
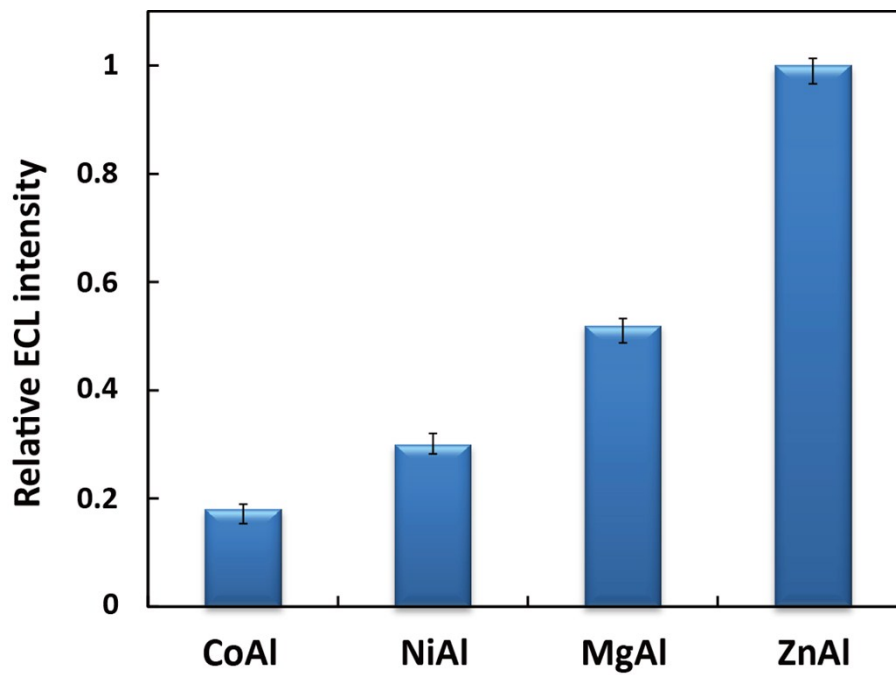
Fig. S10. Relative ECL intensity of PDDA/(Mixture/CoAl-LDH)$_6$, PDDA/(Mixture/NiAl-LDH)$_6$, PDDA/(Mixture/MgAl-LDH)$_6$, PDDA/(Mixture/ZnAl-LDH)$_6$ multilayer films modified glassy carbon electrodes.
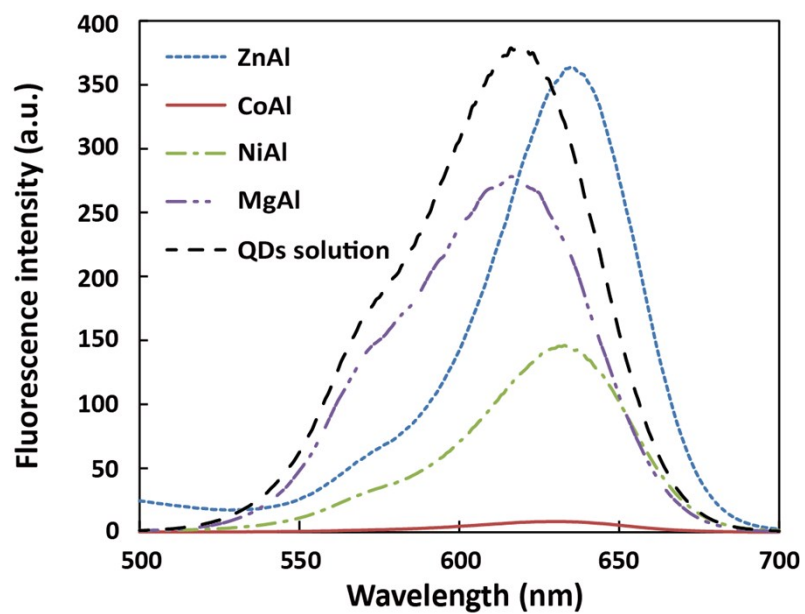
Fig. S11. The fluorescence emission spectra of ZnAl−, CoAl-, NiAl-, MgAl-LDH nanosheets after adsorping an equal amount of CdTe QDs.
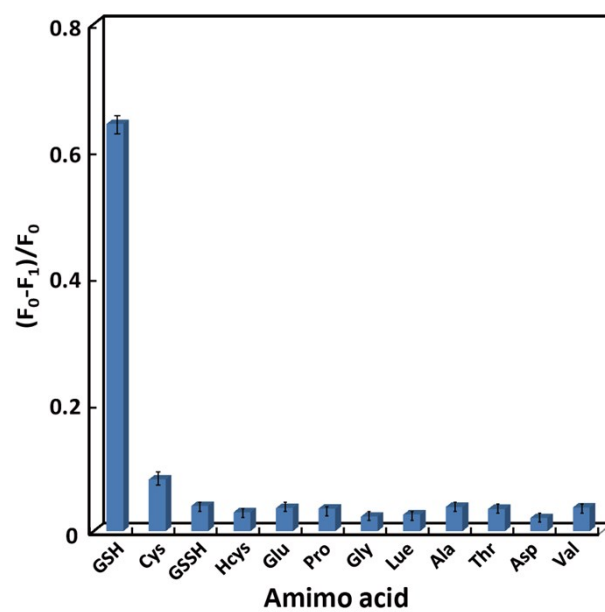
Fig. S12. Selectivity study results of the proposed sensor for the analysis of GSH, the concentration of each interference is 1 μM.
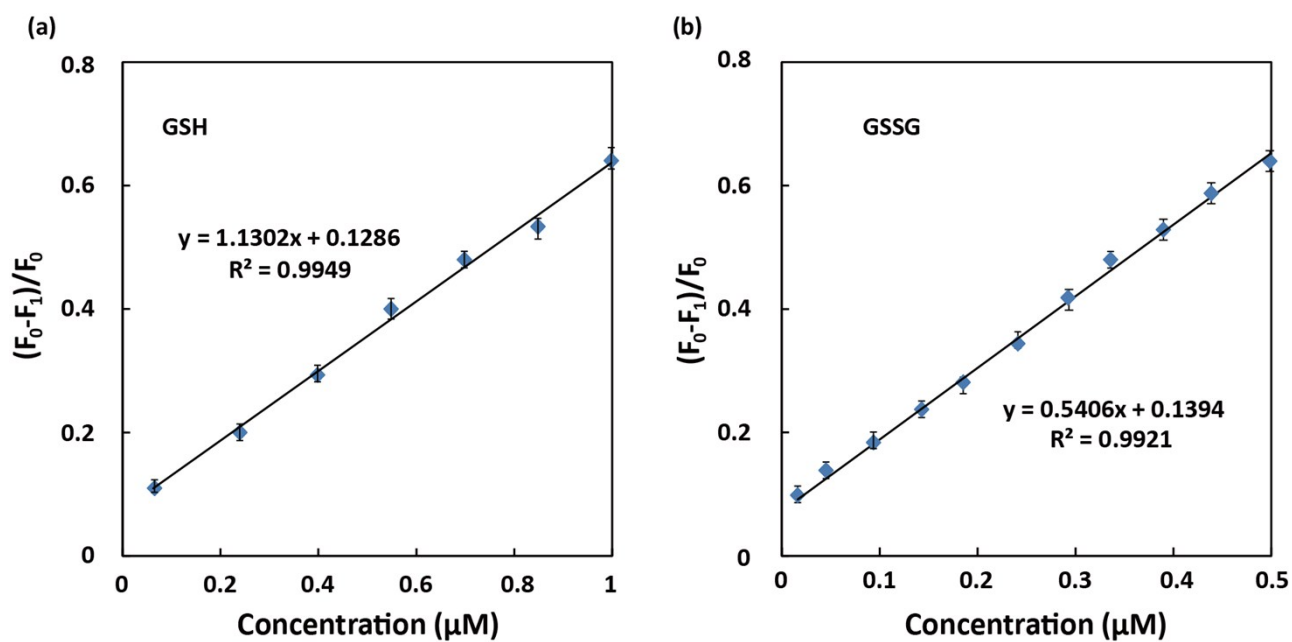
Fig. S13. The calibration curve of (a) GSH or (b) GSSG at PDDA/(Mixture/ ZnAl-LDH)$_6$ multilayer films modified glassy carbon electrodes.
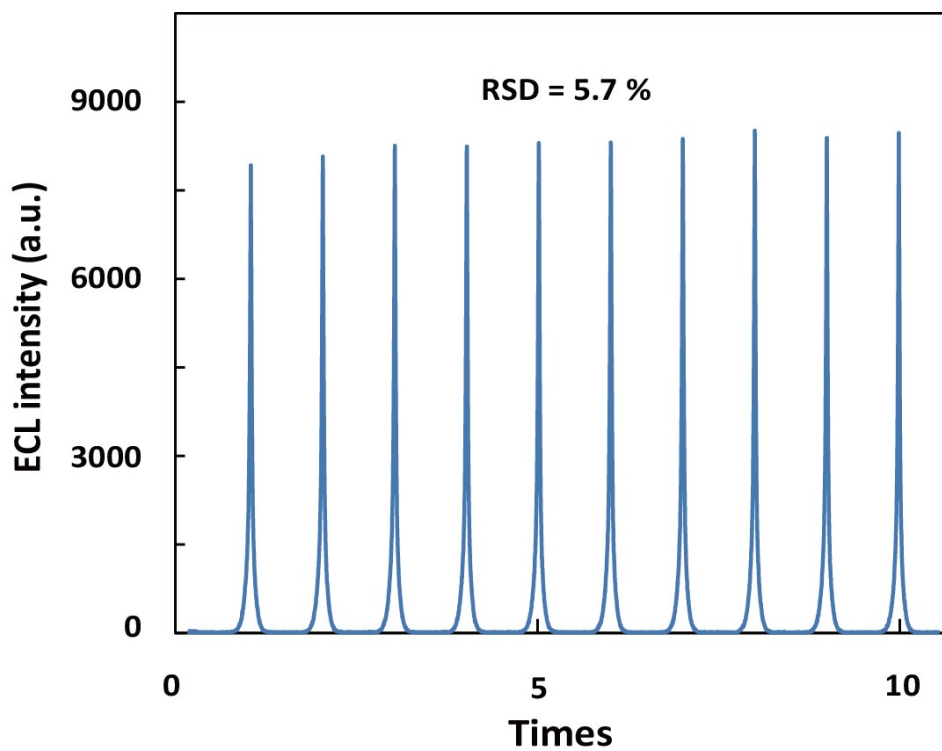
Fig. S14. Consecutive ECL intensities of the PDDA/(Mixture/ZnAl-LDH)$_6$ multilayer films modified GC electrode in 0.1 M PBS solution (pH=7.4) with 50 mM Na$_2$S$_2$O$_8$ and 0.5 μM GSH. Scanning rate: 100 mV/s.